Journal of Asian Earth Sciences 90 (2014) 26–33

Contents lists available at ScienceDirect

Journal of Asian Earth Sciences

journal homepage: www.elsevier.com/locate/jseaes

Curie point depth from spectral analysis of magnetic data in Taiwan

Hsien-Hsiang Hsieh [a,b,c], Chieh-Hung Chen [d], Pei-Ying Lin [c,e], Horng-Yuan Yen [a,*]

[a] Department of Earth Sciences, National Central University, Jhongli, Taiwan, ROC
[b] Institute of Earth Sciences, Academia Sinica, Taipei, Taiwan, ROC
[c] Lamont-Doherty Earth Observatory, Columbia University, Palisades, USA
[d] Department of Earth and Environmental Sciences, National Chung Cheng University, Chiayi, Taiwan, ROC
[e] School of Earth and Space Exploration, Arizona State University, Tempe, AZ, USA

ARTICLE INFO

Article history:
Received 30 September 2013
Received in revised form 31 March 2014
Accepted 8 April 2014
Available online 18 April 2014

Keywords:
Magnetic anomaly
Curie point
Taiwan
Thermal gradient
Heat flow

ABSTRACT

This study constructs an integrated magnetic anomaly map of Taiwan and its vicinity that combines land magnetic data and marine magnetic data. The reduction to pole (RTP) correction method was applied to the integrated magnetic anomaly data. The corrected magnetic anomaly results for a region roughly 880 km in width and 660 km in length fit well with geological tectonic signatures and are used to estimate the Curie point isotherm. The adopted Curie point depth method provides a relationship between the 2-D FFT power spectrum of the magnetic anomalies and the depth of magnetic sources by transforming the spatial data into the frequency domain. The basal depth of the magnetic sources is calculated from the magnetic data. Finally, the Curie point depth of Taiwan is obtained. The highest value of 17 km is located in northern Taiwan, and the lowest value of 6 km is located at southern Taiwan and also has the highest thermal gradient of 88 °C/km. The Curie point depth is consistent with heat-flow measurements with correlation coefficient 0.62.

1. Introduction

The Curie point depth is the theoretical surface with a temperature of approximately 580 °C and can be considered an index of the bottom of a magnetic source, due to ferromagnetic minerals converting to paramagnetic minerals. Geomagnetic anomalies, which are retrieved from magnetic survey, can be utilized to study magnetic structures above the Curie point depth (Bhattacharyya and Leu, 1975a,b; Byerly and Stolt, 1977; Blakely and Hassanzadeh, 1981; Blakely, 1988; Smith and Braile, 1994; Tanaka et al., 1999; Chiozzi et al., 2005; Eppelbaum and Pilchin, 2006; Trifonova et al., 2009; Aboud et al., 2011). Meanwhile, if temperature on the Earth's surface is also taken into account, the geothermal gradient can be constructed from the temperature difference between the Earth's surface and 580 °C, divided by the Curie point depth.

Earlier magnetic studies in Taiwan often focused on regional geological structures, oil–gas exploration, and mineral surveys (Hsieh and Hu, 1972; Wang and Hilde, 1973; Chia and Pan, 1975; Hsiao and Hu, 1978; Yu and Tsai, 1979, 1981; Chang and Hu, 1981; Hu, 1981; Shyu and Chiao, 1983; Hu and Chen, 1986; Liu et al., 1992; Yang et al., 1994; Chen et al., 2001). Other investigations collected regional data and combined them with marine data from oceanic magnetic surveys to construct magnetic anomaly maps in Taiwan's region (Hsu et al., 1998; Wang et al., 2002). However, these magnetic anomaly maps lack data measurements for the Central Range and Coastal Range, due to the difficulty of measuring the violent topography relief on Taiwan Island. To obtain the data distribution for mountainous areas of Taiwan, 11 permanent magnetic stations were built from north to south in Taiwan and utilized as base stations in 2002 (Yen et al., 2004; Chen et al., 2009). Meanwhile, a magnetic survey of the whole island was executed from 2003 to 2004. The land data of over 6000 points covered Taiwan Island well, including plains and ranges every 2 or 7 km. Effects of the diurnal variation at different geo-latitudes were removed from the magnetic data received from the whole island survey, through continuous records of the nearest permanent magnetic station. Earth's main magnetic fields are evaluated by deducting the magnetic field background as given by the International Geomagnetic Reference Field (IGRF). After the diurnal variation, latitude, elevation, and IGRF corrections, all the data points are corrected for magnetic anomalies at the same time and same datum (Yen et al., 2009).

Many tectonic studies have covered Taiwan's seismology (Rau and Wu, 1995; Ma et al., 1996; Kim et al., 2005), GPS (Yu et al., 1999), and geology (Suppe, 1981; Wu et al., 1997; Lin, 2000), but research is lacking on the base tectonic knowledge in the magnetic domain. This study presents an integrated magnetic anomaly map

* Corresponding author. Tel.: +886 03 4227151x65627; fax: +886 03 4222044.
E-mail address: yenhy@earth.ncu.edu.tw (H.-Y. Yen).

http://dx.doi.org/10.1016/j.jseaes.2014.04.007
1367-9120/

combining the latest land magnetic data, including range areas and marine magnetic anomalies, to investigate Taiwan's Curie point depth and thermal gradient.

2. Geological setting

Taiwan is located between the Ryukyu subduction zone to the northeast and the Luzon Arc subduction zone to the south. A young orogeny resulted from the northwestern movements of the Philippine Sea plate (PSP), which intensely interacted with the Eurasian plate (EP). As a result, the strikes of the geological structures in Taiwan are generally in a NNE–SSW direction (Fig. 1). Five major geological zones, Coastal Plain (CP), Western Foothills (WF), Central Range (CR), Longitudinal Valley Fault (LVF), and Coastal Range (CoR), can be identified in Taiwan Island (Chou, 1973). Tertiary rocks dominate the surface geology in Taiwan except for the eastern side of CR, which is exposed with pre-Tertiary metamorphic complexes. The Miocene and earlier type rocks resulting from a former island arc are located east of the metamorphic complex in CoR. LVF separates CoR to the east from CR to the west and is considered a suture that juxtaposes older continental rocks and young island arc materials. CR is composed of three parts: Hsuehshan Range (HR), Backbone Range (BR), and Eastern Central Range (ECR). BR and ECR are composed mainly of slates, and HR is dominated by alternating sandstone and shale layers. CoR is usually thought of as the arc collision from two plates filled with igneous rocks with a high ferromagnetism. WF is composed of Oligocene and Pleistocene clastic sediments stacked by a combination of northwest vergent folds and low-angled thrust faults dipping to the southeast. CP is composed of Quaternary alluvial deposits and Neogene strata underneath.

Two special geological zones, the Kuanying high (KH) and the Peikang high (PH), are located in northwest and west Taiwan, respectively. These are geometric basement highs formed by harder and older rocks. KH is the other prominent basement beneath the northwestern offshore area (Sun and Hsu, 1991). PH

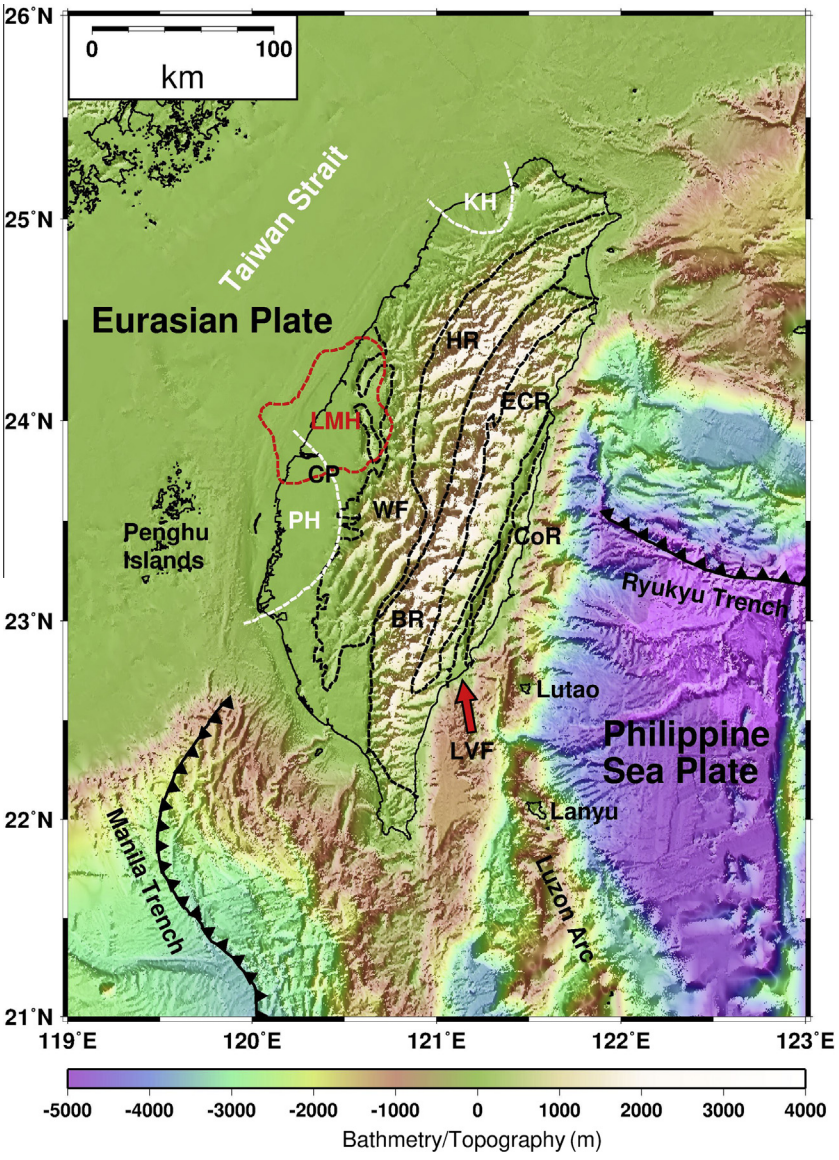

Fig. 1. Topography and geological subdivisions of the Taiwan region. CP: Coastal Plain; WF: Western Foothills; HR: Hsuehshan Range; BR: Backbone Range; ECR: Eastern Central Range; CoR: Coastal Range; LVF: Longitudinal Valley Fault; PH: Peikang High (a geometric basement high); KH: Kuanyin High (a geometric basement high); LMH: Lukang Magnetization High. Manila and Rykukyu Trenches are drawn on the basis of bathymetry only.

is the shallowest pre-Tertiary basement in west Taiwan and is a natural divide between north and south Taiwan.

3. Data

The magnetic anomaly data for land were retrieved from the whole island survey (Yen et al., 2009). To reduce the influence of boundary conditions and edge effects on the calculation of Curie point depth, we included the marine magnetic data, which were modified from the cruises data collected by NGDC, and aeromagnetic data (Hsu et al., 1998). To avoid the high frequency noise caused by tiny structures near ground and coastline, the land magnetic anomalies were combined with marine magnetic anomalies after low-pass filtering. Fig. 2a presents the integrated magnetic anomaly map, which spans 117°E to 125°E and 21°N to 27°N, covering Taiwan and its vicinity and the subduction and collision areas.

4. Methodology

The method that we used to estimate Curie point depth is based on the spectral analysis of magnetic anomaly data. The basic 2-D spectral analysis method was described by Spector and Grant (1970). They estimated the depth to the top of magnetized rectangular prisms (Z_t) from the slope of the log power spectrum. Bhattacharyya and Leu (1975a,b, 1977) further calculated the depth of the centroid of the magnetic source bodies (Z_0). Okubo et al. (1985) developed the method to estimate the bottom depth of the magnetic bodies (Z_b) using the spectral analysis method of Spector and Grant (1970).

Following the method presented by Tanaka et al. (1999), it was assumed that the layer extends infinitely in all horizontal directions. The depth to a magnetic source's upper bound is much smaller than the magnetic source's horizontal scale, and the magnetization $M(x, y)$ is a random function of x and y. Blakely (1995) introduced the power-density spectra of the total-field anomaly $\Phi_{\Delta T}$:

$$\Phi_{\Delta T}(k_x, k_Y) = \Phi_M(k_x, k_Y) \times F(k_x, k_Y), \tag{1a}$$

$$F(k_x, k_Y) = 4\pi^2 C_m^2 |\Theta_m|^2 |\Theta_f|^2 e^{-2|k|Z_t} \left(1 - e^{-|k|(Z_b - Z_t)}\right)^2, \tag{1b}$$

where Φ_M is the power–density spectra of the magnetization, C_m is a proportionality constant, and Θ_m and Θ_f are factors for magnetization direction and geomagnetic field direction, respectively. The equation can be simplified by noting that all terms except $|\Theta_m|^2$ and $|\Theta_f|^2$ are radially symmetric. Moreover, the radial averages of Θ_m and Θ_f are constant. If $M(x, y)$ is completely random and uncorrelated, $\Phi_M(k_x, k_Y)$ is a constant. Hence, the radial average of $\Phi_{\Delta T}$ is

$$\Phi_{\Delta T}(|k|) = A e^{-2|k|Z_t} \left(1 - e^{-|k|(Z_b - Z_t)}\right)^2, \tag{2}$$

where A is a constant and k is the wavenumber. For wavelengths less than about twice the thickness of the layer, Eq. (2) approximately becomes

$$\ln[\Phi_{\Delta T}(|k|)^{1/2}] = \ln B - |k|Z_t, \tag{3}$$

where B is a constant. We could estimate the upper bound of a magnetic source Z_t by fitting a straight line through the high-wavenumber part of a radially averaged power spectrum $\ln[\Phi_{\Delta T}(|k|)^{1/2}]$.

On the other hand, Eq. (2) can be rewritten as

$$\Phi_{\Delta T}(|k|)^{1/2} = C e^{-|k|Z_0} \left(e^{-|k|(Z_t - Z_0)} - e^{-|k|(Z_b - Z_0)}\right), \tag{4}$$

where C is a constant. At long wavelengths, Eq. (4) can be rewritten as

$$\Phi_{\Delta T}(|k|)^{1/2} = C e^{-|k|Z_0} \left(e^{-|k|(-d)} - e^{-|k|(d)}\right) \approx C e^{-|k|Z_0} 2|k|d, \tag{5}$$

where $2d$ is the thickness of the magnetic source. From Eq. (5), it can be concluded that:

$$\ln\left\{\left[\Phi_{\Delta T}(|k|)^{1/2}\right]/|k|\right\} = \ln D - |k|Z_0, \tag{6}$$

where D is a constant. The centroid of the magnetic source Z_0 can be estimated by fitting a straight line through the low-wavenumber part of the radially averaged frequency-scaled power spectrum $\ln\{[\Phi_{\Delta T}(|k|)^{1/2}]/|k|\}$.

From the slope of the power spectrum, the upper bound and the centroid of a magnetic body can be estimated. The lower bound of the magnetic source can be derived (Okubo et al., 1985; Tanaka et al., 1999) as

$$Z_b = 2Z_0 - Z_t. \tag{7}$$

Since Z_b is the lower bound depth of the magnetic body, it suggests that ferromagnetic minerals are converted to paramagnetic minerals due to temperature of approximately 580 °C. Therefore, the obtained bottom depth of the magnetic source, Z_b, was assumed to be the Curie point depth.

In order to relate the Curie point depth (Z_b) to Curie point temperature (580 °C), the vertical direction of temperature variation and the constant thermal gradient were assumed. The geothermal gradient (dT/dz) between the Earth's surface and the Curie point depth (Z_b) can be defined by Eq. (8) (Tanaka et al., 1999; Stampolidis et al., 2005; Maden, 2010):

$$dT/dz = 580^{\circ}\mathrm{C}/Z_b. \tag{8}$$

Further, the geothermal gradient can be related to the heat flow q by using the formula (Turcotte and Schubert, 1982; Tanaka et al., 1999):

$$q = \lambda(dT/dz) = \lambda(580^{\circ}\mathrm{C}/Z_b). \tag{9}$$

where λ is the coefficient of thermal conductivity. From Eq. (9), the Curie point depth is inversely proportional to heat flow.

5. Curie point depth estimates for Taiwan

The magnetic anomalies measured on the Earth's surface, in which the Earth's main field has been removed, result from underlying magnetic materials due to susceptibility. The inclination and the declination of the Earth's main field dominate the magnetic anomalies of the induction field. The correction of reduction to pole (RTP) is often applied to the magnetic anomalies to obtain corrected maps of magnetic anomaly values induced by the inclination of 90° and the declination of 0°. Thus, the anomaly values in corrected maps are with respect to magnetic materials, which lie vertically below. The traditional RTP method (Baranov, 1957) is usually used in areas at the middle or high magnetic latitudes. Taiwan is located at about 22°N–26°N. Cooper and Cowan (2005) developed the RTP method, which is better suited to Taiwan and its vicinity. The integrated magnetic data of Fig. 2a were reduced to the North magnetic pole. The corrected reduction to pole anomaly map of Taiwan is shown in Fig. 2b.

The corrected map (Fig. 2b) spanning roughly 880 km in the E–W direction and 660 km in the N–S direction was the input for the Curie point depth analysis. The depth simulations suggest that the optimal square window dimension is about 10 times the estimated depth (Chiozzi et al., 2005). Thus, the map was subdivided into square subregions of 250 km × 250 km. These subregions are shifting with respect to each other in increments of 10 km. The 2-D FFT power spectrum method (Eqs. (3) and (6)) was applied to each subregion. Z_0, the centroid depth of magnetic sources, and Z_t, the top depth of magnetic sources, were derived from the slopes of the longest and second-longest wavelengths of the frequency-scaled power spectrum $\ln\{[\Phi_{\Delta T}(|k|)^{1/2}]/|k|\}$ and the radially

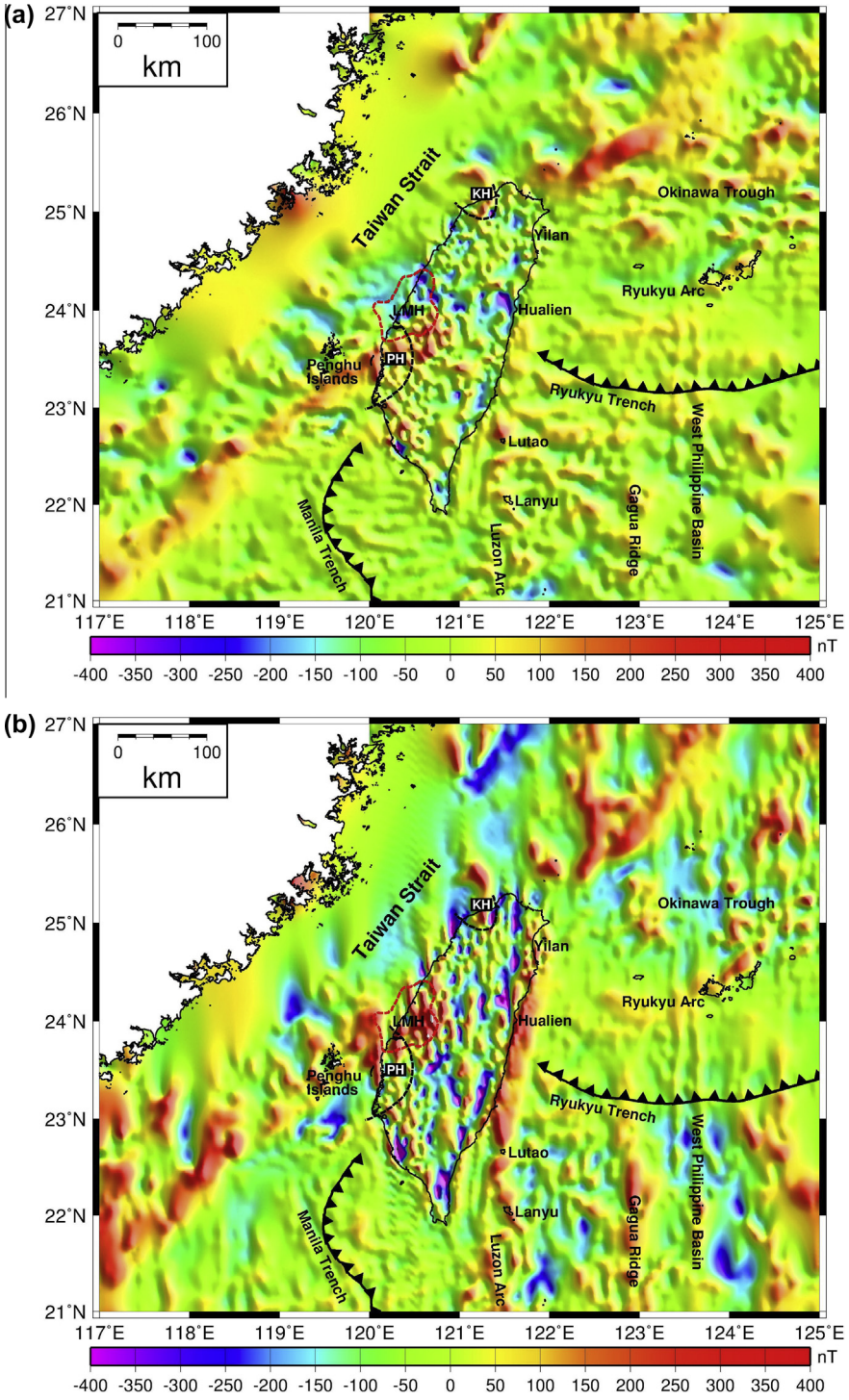

Fig. 2. (a) Integrated magnetic anomaly map of Taiwan and vicinity; (b) corrected magnetic anomaly map of Taiwan and vicinity.

averaged power spectrum $\ln[\Phi_{\Delta T}(|k|)^{1/2}]$, respectively. An example of the estimates in a subregion is shown in Fig. 3. Because the computation requires an extensive dataset and the magnetic data do not cover the entire area, we considered the missing-data area in the northwest corner of the map and the crustal materials sharply change between land and marine areas. The analysis of Curie point depth was only along the central part of the investigated area (Taiwan Island). The centers of subregions are marked with signs in Fig. 4a. Here, the Curie point depth (Z_b) of Taiwan was derived from Eq. (7) (Fig. 4a).

6. Interpretations and analytical results

In the corrected map (Fig. 2b), the positive anomaly belt in the SW–NE direction along Penghu Islands in the Taiwan Strait and extending into Taiwan Island is further north than in the integrated anomaly map (Fig. 2a). The positive anomaly is considered the continental boundary of EP and is consistent with the location of the basalt rocks near Penghu Islands (Chung et al., 1994; Hsieh et al., 2010) and the Lukang Magnetization High (LMH) structure (Hsu et al., 2008). The other belt shape with a positive anomaly on the

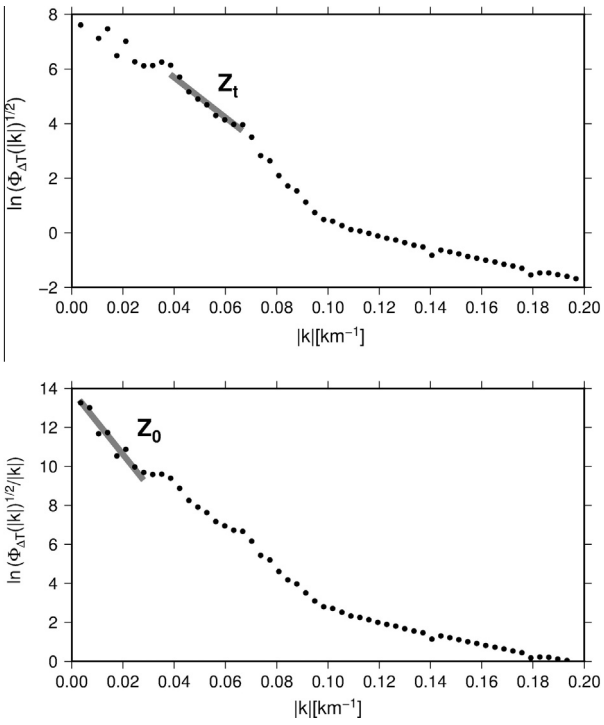

Fig. 3. Example of spectra for the estimation of (a) the depth of the top bound (Z_t) and (b) the depth of the centroid (Z_0) of magnetic sources.

eastern side of Taiwan on the corrected map is from south (Lanyu and Lutao) to north (Hualien and Yilan) and fits well the Luzon arc formed by EP subducting to PSP due to igneous rocks with a high ferromagnetic property. The other high anomalies appear over Ryuku Arc and Gagua Ridge, which are igneous structures. Relatively low anomalies were found in Okinawa Trough and West Philippine Basin that suggest existence of sedimentary rocks. On Taiwan Island, the positive and negative anomalies were observed in two geometric basement highs (i.e., PH and KH) and LVF as well as basins, respectively. The positive and negative anomalies in mountain areas show the regional geology resulting from orogeny and metamorphism.

The Curie point depth (Z_b) map of Taiwan (Fig. 4a) shows that the depth ranged from 17 km in northern Taiwan to 6 km in southern Taiwan. The depths are between the ranges of continent and island arc areas (Bhattacharyya and Morley, 1965; Okubo et al., 1989; Tanaka et al., 1999), except for the shallowest part in southern Taiwan. Z_b increasing from 9 to 14 km along the E–W direction, which is similar to the topography relief exception in west-southern CR. High Z_b values are observed in KH (15 km), PH (14 km), LMH (12–13 km), and northern Taiwan (16 km). By contrast, shallow Z_b values are located beneath the southern Central Range (9–10 km) and southern Taiwan (6–9 km).

The geothermal gradient map of Taiwan (Fig. 4b) was estimated from Eq. (8). The contours are roughly consistent with the newest measured geothermal gradient data for Taiwan (Wu et al., 2013). The higher geothermal gradient areas are all beneath CR and the eastern side of Taiwan, especially in southern CR and CoR. High geothermal gradients (from 60 to 72 °C/km) are mainly distributed in the southwestern and on the eastern side of CR. The highest geothermal gradient (88 °C/km) is at the southern end of Taiwan Island. Lower geothermal gradient areas are at northern and western Taiwan from 36 to 52 °C/km, which is higher than the average geothermal gradient observed in continents. The shallow Curie depths (9–12 km) beneath CR and WF with higher thermal gradient (52–64 °C/km) indicate activity from young orogeny and plates, resulting in frequent, pronounced temperature change, especially beneath south CR.

The heat-flow values using Curie point depth for Taiwan (Fig. 4c) were derived from Eq. (9) with the average thermal conductivity $\lambda = 2.978\ \mathrm{Wm^{-1}\ K^{-1}}$) calculated from Wu et al. (2013). The analytical heat-flow results (Fig. 4c) from the Curie point depth and geothermal gradient are in high agreement with the measured heat flow map of Taiwan (Fig. 5) (Lee and Cheng, 1986; Lin, 2000), with regard to the shape of the contours. The high heat flow values along the eastern side of Taiwan beneath the boundaries of two plates (LVF) may be produced by the plate activities of collision and subduction. Comparing Z_b with the heat flow values retrieved

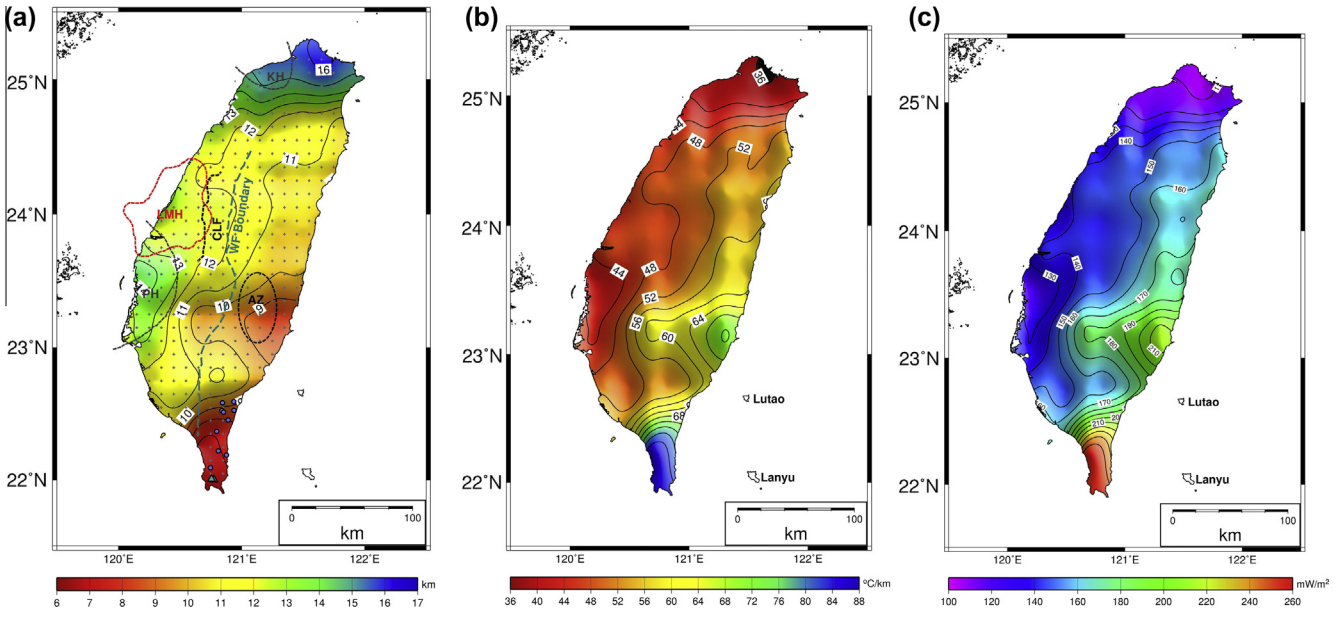

Fig. 4. (a) Curie point depth (Z_b) map (+: CPD estimate points; circle: hot springs; triangle: mud volcanoes; ellipse: Aseismic Zone (AZ); green line: WF boundary; black line: Chelungpu Fault); (b) thermal gradient map derived from Curie point depth map (Curie temperature 580 °C); (c) heat flow map derived from Curie point depth (thermal conductivity 2.978 $\mathrm{Wm^{-1}\ K^{-1}}$).

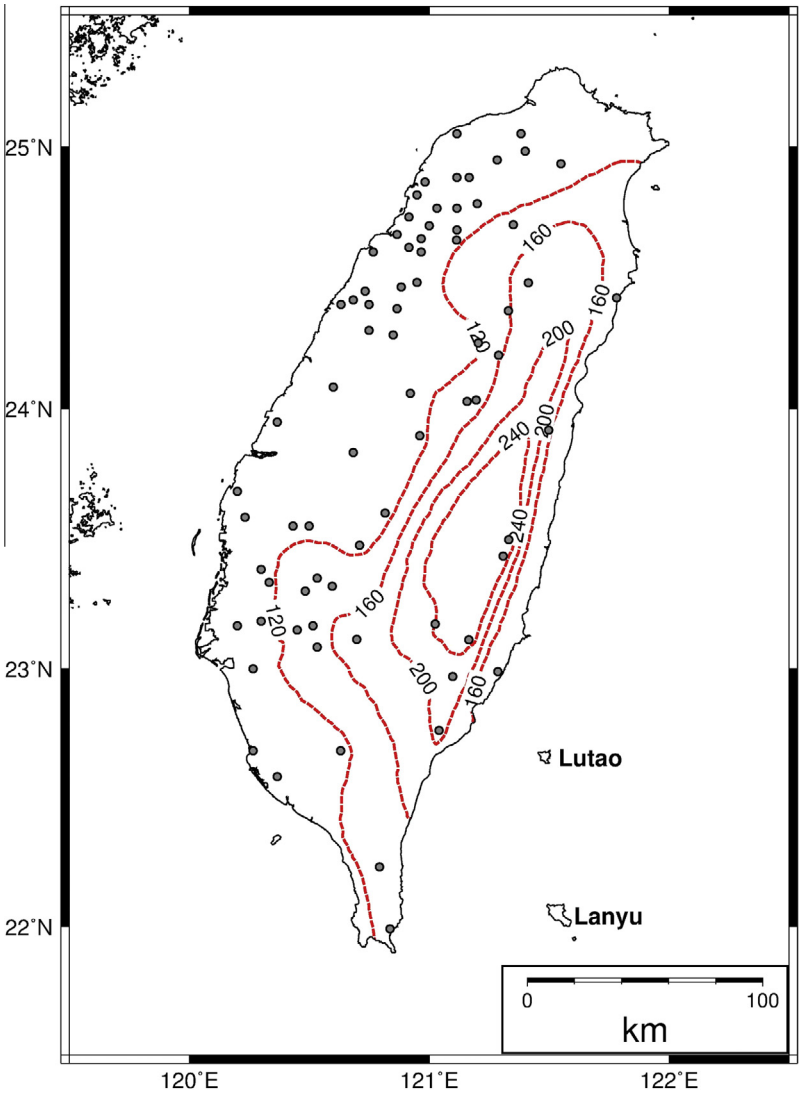

Fig. 5. Heat flow map (mW/m^2) of Taiwan, redrawn from Lee and Cheng (1986) and Lin (2000).

from the survey results (Lee and Cheng, 1986; Lin, 2000) yielded a linear relationship with a correlation coefficient of 0.62 (Fig. 6), which suggests that Z_b is highly related to the heat flow measurements.

PH in the western continental margin where the pre-Miocene basement extends from the Penghu Islands to western Taiwan (Lin et al., 2003) plays an important role in the orogenic evolution of Taiwan. PH with relatively high Curie point depth (CPD) and low geothermal gradient, presenting cooler and harder structures as a stiff crustal obstacle, underlay west-southern Taiwan. It suggests that PH resists the push from plate collisions to develop the kinematics of a fold-and-thrust system in the upper crust located at WF and CP (Mouthereau et al., 2002). KH is also showing the relatively cool and hard structures in west-northern Taiwan, although at a smaller scale. LMH with a high magnetic anomaly (400 nT) and deep Z_b (12–13 km) resulted from rocks with high susceptibility. The shallow Z_b (9 km) and high geothermal gradient (64–72 °C/km) appearing at south CoR might have been caused by the north Luzon arc's inserting under CoR and encountering the Chengguang'ao igneous rocks underneath. The Z_b (6–9 km) in southern Taiwan reflects the extremely strong and active thermal activities with geothermal gradient (68–88 °C/km), which is confirmed by the distribution of hot springs and mud volcanoes (Fig. 4a) and geothermal measurements made by Industrial Technology Research Institute of Taiwan (ITRI) in 2012 using surface well logging.

The boundaries of WF and CR are along CPD contours (12 km). The trend of CPD in west-central Taiwan increases toward the west across the Chelungpu Fault (CLF). The CLF system has been delineated by Wang et al. (2000) from a seismic experiment, as shown in Fig. 4a along the right border of LMH. CPD variation is found across the CLF system, with shallower depth in the hangingwall than in the footwall (Fig. 4a). This means that the geothermal gradient is higher in the hangingwall than in the footwall. Even though this is a small-scale feature, the geothermal gradient's changing along both sides of CLF are close to the pre-Neogene basement at depths of about 8–10 km (Wang et al., 2002) and the depth of Q_p variation across the fault system (Wang et al., 2010).

As mentioned by Yen et al. (2009), the high magnetic anomaly also corresponds to the aseismic zone from seismological observations (Ma et al., 1996; Lin, 1998) beneath southern CR. The aseismic zone is within a region of low Vp/Vs, around 1.6 (Kim et al., 2005; Wu et al., 2007), and a region of high Q_p/Q_s, around 1.2–1.4 (Wang et al., 2010). The present work also indicated shallow Curie point depth (9–10 km), high geothermal gradient (60–64 °C/km), and high heat flow value (200–240 mW/m^2) (Lee and Cheng, 1986; Wu et al., 2013). These results all relate the

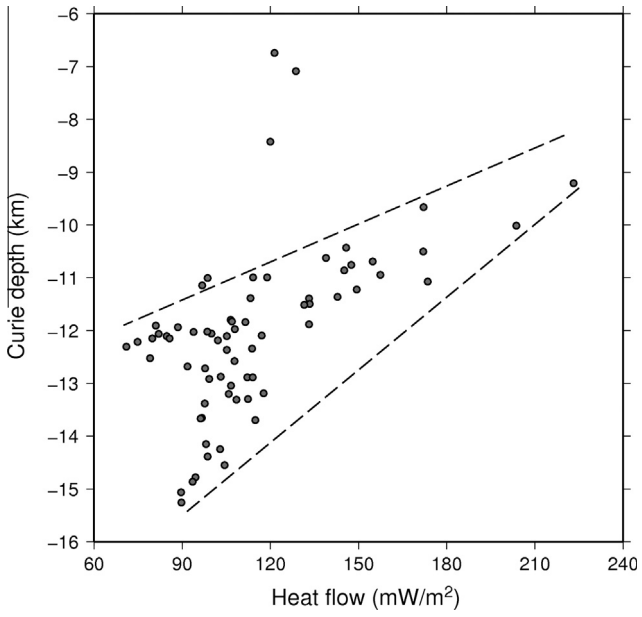

Fig. 6. Relationship between Curie point depth from magnetic data and heat flow data from well measurements. The linear correlation coefficient is 0.62.

possible extra-heat and dry tectonic structures by plates collision and subduction (Lin, 2000; Yamato et al., 2009). The CPD map shows the parallel strikes along the topography and geological zone (LVF) in eastern Taiwan. The suture belt between PSP and EP shows shallow CPD (10–11 km) with higher geothermal gradient and higher heat flow values that indicate violent plate activity.

7. Conclusions

The integrated and corrected magnetic anomaly maps (Fig. 2) were modified by land and oceanic data combination. The Curie point depth (Z_b) was estimated by spectral analysis of magnetic anomaly data of Taiwan and its vicinity. The present result was compared with the tectonic and heat flow data. The Z_b map (Fig. 4a) shows the Curie point depth of Taiwan from 6 to 17 km. The Curie point depth indicates the bottom depth of magnetic sources and reflects the thermal gradient and the observed heat flow data. The thermal gradient map of Taiwan (Fig. 4b) shows that the thermal gradient varies from 36 °C/km to 88 °C/km. Comparing the Curie point depth map with the heat flow map of Taiwan (Fig. 6), the linear relationship between magnetic data and heat flow survey had a correlation coefficient of 0.62. High heat flow values were observed at the boundaries of continent-arc regions in eastern Taiwan and in geological thermal areas at southern Taiwan where Curie point depths are shallow, whereas deep Curie point depths are located at two geometric basement highs (PH and KH) in western and northern Taiwan where thermal gradients and heat flows are low. The results show that the Curie point depths of Taiwan are shallower than about 11 km at mud volcanoes, geothermal areas, and plate activity boundaries and 13–16 km at older and cooler continental edges.

Acknowledgements

We special thank Chi, Wu-Cheng for making available the heat flow data and Hsu, Shu-Kun for making available the marine magnetic data. And everyone offered efforts for land magnetic data surveys.

References

Aboud, E., Salem, A., Mekkawi, M., 2011. Curie depth map for Sinai Peninsula, Egypt deduced from the analysis of magnetic data. Tectonophysics 506, 46–54.
Baranov, V., 1957. A new method for interpretation of aeromagnetic maps: Pseudo-gravimetric anomalies. Geophysics 22, 359–383.
Bhattacharyya, B.K., Leu, L.K., 1975a. Analysis of magnetic anomalies over yellowstone national park: mapping and curie point isothermal surface for geothermal reconnaissance. J. Geophys. Res. 80, 4461–4465.
Bhattacharyya, B.K., Leu, L.K., 1975b. Spectral analysis of gravity and magnetic anomalies due to two-dimensional structures. Geophysics 40, 993–1013.
Bhattacharyya, B.K., Leu, L.K., 1977. Spectral analysis of gravity and magnetic anomalies due to rectangular prismatic bodies. Geophysics 42, 41–50.
Bhattacharyya, B.K., Morley, L.W., 1965. The delineation of deep crustal magnetic bodies from total field aeromagnetic anomalies. J. Geomagn. Geoelectr. 17, 237–252.
Blakely, R.J., 1988. Curie temperature isotherm analysis and tectonic implications of aeromagnetic data from Nevada. J. Geophys. Res. 93, 817–832.
Blakely, R.J., 1995. Potential Theory in Gravity and Magnetic Applications. Cambridge University Press, Cambridge.
Blakely, R.J., Hassanzadeh, S., 1981. Estimation of depth to magnetic source using maximum entropy power spectra with application to the Peru–Chile trench. Geol. Soc. Am. Mem. 154, 667–681.
Byerly, P.E., Stolt, R.H., 1977. An attempt to define the Curie point isotherm in northern and central Arizona. Geophysics 42, 1394–1400.
Chang, S.L., Hu, C.C., 1981. Gravity and magnetic anomalies of Taiwan and their tectonic implication. Mem. Geol. Soc. China 4, 121–142.
Chen, K.J., Wang, C.M., Hsu, S.K., Liang, W.T., 2001. Geomagnetic basement relief of the northern Taiwan area. Terr. Atmos. Oceanic Sci. 12, 441–460.
Chen, C.H., Lin, C.R., Chao, H.L., Yen, H.Y., Liu, J.Y., Yeh, Y.H., 2009. Evaluation of the applicability of Chapman-Miller method on variation of the geomagnetic total intensity field in Taiwan from 1988 to 2007. Terr. Atmos. Oceanic Sci. 20 (6), 799–806.
Chia, H.S., Pan, Y.S., 1975. The magnetic model study of the northwest offshore of Taiwan. Petrol. Geol. Taiwan 12, 131–144.
Chiozzi, P., Matsushima, J., Okubo, Y., Pasquale, V., Verdoya, M., 2005. Curie-point depth from spectral analysis of magnetic data in central–southern Europe. Phys. Earth Planet. Inter. 152, 267–276.
Chou, J.T., 1973. Sedimentology and paleogeography of the upper Cenozoic system of western Taiwan. Proc. Geol. Soc. China 16, 111–144.
Chung, S.L., Sun, S., Tu, K., Chen, C.H., Lee, C.Y., 1994. Late Cenozoic basaltic volcanism around the Taiwan Strait, SE China: product of lithosphere-asthenosphere interaction during continental extension. Chem. Geol. 112, 1–20.
Cooper, G.R.J., Cowan, D.R., 2005. Differential reduction to the pole. Comput. Geosci. 31, 989–999.
Eppelbaum, L.V., Pilchin, A.N., 2006. Methodology of Curie discontinuity map development for regions with low thermal characteristics: an example from Israel. Earth Planet. Sci. Lett. 243 (3-4), 536–551.
Hsiao, P.T., Hu, C.C., 1978. Geomagnetic study of the Changhua plain, Taiwan. Petrol. Geol. Taiwan 15, 241–254.
Hsieh, S.H., Hu, C.C., 1972. Gravity and magnetic studies of Taiwan. Petrol. Geol. Taiwan 10, 283–321.
Hsieh, H.H., Yen, H.Y., Shih, M.H., 2010. Moho depth de rived from grav ity data in the Tai wan Strait area. Terr. Atmos. Ocean Sci. 21, 235–241.
Hsu, S.K., Liu, C.S., Shyu, C.T., Liu, S.Y., Sibuet, J.C., Lallemand, S., Wang, C., Reed, D., 1998. New gravity and magnetic anomaly maps in the Taiwan-Luzon region and their preliminary interpretation. Terr. Atmos. Oceanic Sci. 9, 509–532.
Hsu, S.K., Yeh, Y.C., Lo, C.L., Lin, A.T., Doo, W.B., 2008. Link between crustal magnetization and earthquakes in Taiwan. Terr. Atmos. Oceanic Sci. 19, 445–450.
Hu, C.C., 1981. Gravity and magnetic studies of Taoyuan and Hsinchu area. Bull. Geophys. Natl. Central Univ. 21, 49–60.
Hu, C.C., Chen, W.S., 1986. Gravity and magnetic anomalies of eastern Taiwan. Mem. Geol. Soc. China 7, 341–352.
Kim, K.H., Chiu, J.M., Pujo, J., Chen, K.C., Huang, B.S., Yeh, Y.H., Shen, P., 2005. Three-dimensional VP and VS structural models associated with the active subduction and collision tectonics in the Taiwan region. Geophys. J. Int. 162, 204–220.
Lee, C.R., Cheng, W.T., 1986. Preliminary heat flow measurements in Taiwan. Fourth Circum Pacific Energy and Mineral Resources Conference, Singapore.
Lin, C.H., 1998. Tectonic implications of an aseismic belt beneath the Eastern Central Range of Taiwan: crustal subduction and exhumation. J. Geol. Soc. China 41, 441–460.
Lin, C.H., 2000. Thermal modeling of continental subduction and exhumation constrained by heat flow and seismicity in Taiwan. Tectonophysics 324, 189–201.
Lin, A.T., Watts, A.B., Hesselbo, S.P., 2003. Cenozoic stratigraphy and subsidence history of the South China Seamargin in the Taiwan region. Basin Res. 15, 453–478.
Liu, C.S., Liu, S.Y., Kuo, B.Y., Lundberg, N., Reed, D.L., 1992. Characteristics of the gravity and magnetic anomalies off southern Taiwan. ACTA Geol. Taiwanica Sci. Rep. Natl. Taiwan Univ. 30, 123–130.
Ma, K.F., Wang, J.H., Zhao, D., 1996. Three-dimensional seismic velocity structure of the crust and uppermost mantle beneath Taiwan. J. Phys. Earth 44 (2), 85–105.
Maden, N., 2010. Curie-point depth from spectral analysis of magnetic data in Erciyes stratovolcano (Central TURKEY). Pure Appl. Geophys. 167, 349–358.

Mouthereau, F., Deffontaines, B., Lacombe, O., Angelier, J., 2002. Variations along the strike of the Taiwan thrust belt: basement control on structural style, wedge geometry, and kinematics. Geology and Geophysics of an Arc-Continent Collision, Taiwan, Republic of China, vol. 358. Geological Society of America Special Paper, pp. 35–58.

Okubo, Y., Graf, R.J., Hansen, R.O., Ogawa, K., Tsu, H., 1985. Curie point depths of the island of Kyushu and surrounding areas, Japan. Geophysics 50, 481–494.

Okubo, Y., Tsu, H., Ogawa, K., 1989. Estimation of Curie point temperature and geothermal structure of island arcs of Japan. Tectonophysics 159, 279–290.

Rau, R.J., Wu, F.T., 1995. Tomographic imaging of lithospheric structures under Taiwan. Earth Planet. Sci. Lett. 133, 517–532.

Shyu, C.T., Chiao, L.Y., 1983. Trends of magnetic anomalies in the immediate offshore area of the I-Lan Plain, Taiwan. ACTA Oceanographica Taiwanica 14, 16–25.

Smith, R.B., Braile, L.W., 1994. The Yellowstone Hotspot, 3. J. Volcanol. Geotherm. Res. 61, 121–187.

Spector, A., Grant, F.S., 1970. Statistical models for interpreting aeromagnetic data. Geophysics 35, 293–302.

Stampolidis, A., Kane, I., Tsokas, G.N., Tsourlos, P., 2005. Curie point depths of Albania inferred from ground total field magnetic data. Surv. Geophys. 26, 461–480.

Sun, S.C., Hsu, Y.Y., 1991. Overview of the Cenozoic geology and tectonic development of offshore and onshore Taiwan. Taicrust Workshop Proc., 35–47.

Suppe, J., 1981. Mechanics of mountain building and metamorphism in Taiwan. Mem. Geol. Soc. China 4, 67–89.

Tanaka, A., Okubo, Y., Matsubayashi, O., 1999. Curie point depth based on spectrum analysis of the magnetic anomaly data in East and Southeast Asia. Tectonophysics 306, 461–470.

Trifonova, P., Zhelev, Z., Petrova, T., Bojadgieva, K., 2009. Curie point depth of Bulgarian territory infered from geomagnetic observations and its correlation with regional termal structure and seismicity. Tectonophysics 473, 362–374.

Turcotte, D.L., Schubert, G., 1982. Geodynamics. Cambridge University Press, New York.

Wang, C., Hilde, T.W.C., 1973. Geomagnetic interpretation of the geologic structure in the northeast offshore region of Taiwan. ACTA Oceanographica Taiwanica 3, 141–156.

Wang, C.Y., Chang, C.H., Yen, H.Y., 2000. An Interpretation of the 1999 Chi-Chi Earthquake in Taiwan based on the thin-skinned thrust model. Terr. Atmos. Ocean 11, 609–630.

Wang, C., Huang, C.P., Ke, L.Y., Chien, W.J., Hsu, S.K., Shyu, C.T., Cheng, W.B., Lee, C.S., Teng, L.S., 2002. Formation of the Taiwan island as a solitary wave the Eurasian Continental Plate margin: magnetic and seismological evidence. Terr. Atmos. Ocean Sci. 13, 339–354.

Wang, Y.J., Ma, K.F., Mouthereau, F., Eberhart-Phillips, D., 2010. Three-dimensional *Qp*- and *Qs*-tomography beneath Taiwan orogenic belt: implications for tectonic and thermal structure. Geophys. J. Int. 180, 891–910.

Wu, F.T., Rau, R.J., Salzberg, D., 1997. Taiwan orogeny: thin-skinned or lithospheric collision? Tectonophysics 274, 191–220.

Wu, Y.M., Chang, C.H., Zhao, L., Shyu, J.B.H., Chen, Y.G., Sieh, K., Avouac, J.P., 2007. Seismic tomography of Taiwan: improved constraints from a dense network of strong motion stations. J. Geophys. Res. 112, B08312.

Wu, S.K., Chi, W.C., Hsu, S.M., Ke, C.C., Wang, Y., 2013. Shallow crustal thermal structures of central Taiwan foothills region. Terr. Atmos. Ocean Sci. 24, 695–707.

Yamato, P., Mouthereau, F., Burov, E., 2009. Taiwan mountain building: insights from 2D thermo-mechanical modelling of a rheologically-stratified lithosphere. Geophys. J. Int. 176, 307–326.

Yang, C.H., Shei, T.C., Lue, C.C., 1994. Gravity and magnetic studies in the Tatun Volcanic region. Terr. Atmos. Ocean Sci. 5, 499–514.

Yen, H.Y., Chen, C.H., Yeh, Y.H., Liu, J.Y., Lin, C.R., Tsai, Y.B., 2004. Geomagnetic fluctuations during the 1999 Chi–Chi earthquake in Taiwan. Earth Planets Space 56, 39–45.

Yen, H.Y., Chen, C.H., Hsieh, H.H., Lin, C.R., Yeh, Y.H., Tsai, Y.B., Liu, J.Y., Yu, G.K., Chen, Y.R., 2009. Magnetic survey of Taiwan and its preliminary interpretations. Terr. Atmos. Ocean Sci. 20 (2), 309–314.

Yu, S.B., Tsai, Y.B., 1979. Geomagnetic anomalies of the Ilan plain, Taiwan. Petrol. Geol. Taiwan 16, 19–27.

Yu, S.B., Tsai, Y.B., 1981. Geomagnetic investigations in the Pongtung plain, Taiwan. Bull. Inst. Earth Sci. Acad. Sin. 1, 189–208.

Yu, S.B., Kuo, L.C., Punongbayan, R.S., Ramos, E.G., 1999. GPS observation of crustal motion in the Taiwan-Luzon region. Geophys. Res. Lett. 26 (7), 923–926.